ISSN 1067-8212, Russian Journal of Non-Ferrous Metals, 2009, Vol. 50, No. 5, pp. 474–484. © Allerton Press, Inc., 2009.

PHYSICAL METALLURGY AND HEAT TREATMENT

Phase Transformation, Structural Evolution and Mechanical Property of Nanostructured FeAl as a Result of Mechanical Alloying[1]

M. M. Rajath Hegde and A. O. Surendranathan

Department of Metallurgical and Materials Engineering, NITK Surathkal, Srinivasanagar – 575025, Dakshina Kannada, Karnataka, India

e-mail: rajathhegdemm63@yahoo.co.in; aos_nathan54@yahoo.com.au

Abstract—Objective of the work was to synthesize **nanostructured** FeAl alloy powder by mechanical alloying (MEA). The work concentrated on synthesis, characterization, structural and mechanical properties of the alloy. Nanostructured FeAl intermetallics were prepared directly by MEA in a high energy rate ball mill. Milling was performed under **toluene** solution to avoid contamination from the milling media and atmosphere. Mixtures of elemental Fe and Al were progressively transformed into a partially disordered solid solution with an average composition of Fe—50 at % Al. Phase transformation, structural changes, morphology, particle size measurement and chemical composition during MEA were investigated by X-ray diffraction (XRD), Scanning electron microscopy (SEM) and Energy dispersive X-ray spectroscopy (EDS) respectively. Vickers micro hardness (VMH) indentation tests were performed on the powders. XRD and SEM studies revealed the alloying of elemental powders as well as transition to nanostructured alloy, crystallite size of 18 nm was obtained after 28 hours of milling. Expansion/contraction in lattice parameter accompanied by reduction in crystallite size occurs during transition to nanostructured alloy. Longer milling duration introduces ordering in the alloyed powders as proved by the presence of superlattice reflection. Elemental and alloyed phase coexist while hardness increased during MEA.

Key words: Nanostructured Powder; Mechanical Alloying; FeAl; Disorder; Order; Ball Milling.

DOI: 10.3103/S1067821209050095

1. INTRODUCTION

1.1. Nanomaterials—Definition and Properties

Although a broad definition, nanomaterials are categorised as those which have structured components with at least one dimension less than 100 nm. Materials that are nanoscale in three dimensions are particles, for example precipitates, colloids and quantum dots (tiny particles of semiconductor materials). **Nanocrystalline materials**, made up of nanometre-sized grains, also fall into this category. Two principal factors cause the properties of nanomaterials to differ significantly from other materials: increased relative surface area, and quantum effects. These factors can change or enhance properties such as reactivity, strength and electrical characteristics. For materials such as crystalline solids, as the size of their structural components decreases, there is much greater interface area within the material, this can greatly affect both mechanical and electrical properties. For example, most metals are made up of small crystalline grains, the boundaries between the grains slow down or arrest the propagation of defects when the material is stressed, thus giving it strength. If these grains can be made very small, or even nanoscale in size, the interface area within the material greatly increases, which enhances its strength. For example, nanocrystalline nickel is as strong as hardened steel.

1.2. FeAl Alloy

The FeAl intermetallic compound offers a combination of attractive properties such as a high specific strength, good strength at intermediate temperatures and an excellent corrosion resistance at elevated temperatures under oxidizing, carburizing and sulfidizing atmospheres. So they have attracted considerable attention as potential candidates for structural and coating applications at elevated temperatures in hostile environments and as promising substitutes for stainless steels at room temperatures. FeAl intermetallic represents a new approach in the permanent magnets used in electrical motors, these motors are used in electric vehicles and gasoline vehicles. The soft magnetic core is an important segment of the permanent magnet used in these electric motors. Using powder metallurgy technique in developing a soft magnetic FeAl core will replace silicon irons or phosphorous irons presently used in the cores of permanent magnets. FeAl alloys are expected to be lighter, cheaper and offer improved electrical, mechanical and magnetic properties than the cur-

[1] The article is published in the original.

rent alloys. However, these alloys have been limited by their low ductility at room temperature and low mechanical strength above 600°C. The need is to impart improved mechanical properties by reducing the crystallite size to the nanometer range.

Efforts have been focused to synthesize ultrafine FeAl intermetallic powder by mechanical alloying (MEA), with grain size in the nanoscale regime. Mechanical alloying technique as a function of high energy rate ball milling is utilized to alloy the elemental powder as well as to reduce the crystallite size.

1.3. Mechanical Alloying (MEA)

Mechanical alloying (MEA) in a high energy rate ball mill is a practical processing route for the synthesis of phases or phase mixtures. The process leads to an alloy formation by solid state reactions assisted by severe plastic deformation that occurs during ball milling of the elemental powders. The MEA technique allows one to overcome problems such as e.g., that associated with large difference in melting points of the alloying components as well as unwanted segregation or evaporation that could occur during melting and casting. In addition nanocrystalline structures can be formed by MEA process. When ordered Fe-40Al was subjected to ball milling, three types of structural changes occurred: nanocrystallisation, loss of long range order (LRO) and destruction of chemical short range order (CSRO) [1]. A new nanostructured system, FeAlB, with high content of boron, was prepared by mechanical alloying in a high energy rate ball mill, structural and magnetic properties were investigated [2]. In the recent past, there have been many reports about MEA of Fe-50 at % Al [3–6].

Structural and phase transformations occurred during the mechanical alloying (as a result of ball milling) of Fe-50 at % Al nano powder mixture and during subsequent heating of the milled nano powders have been reported [7]. The disordered Fe(Al) solid solution is the product of the milling process in all the above mentioned cases. Fully ordered FeAl phase obtained by MEA of Fe-50 at % Al has been reported [8]. A metastable, nanocrystalline Fe-66Al solid solution, which is ferromagnetic at room temperature, was prepared from elemental powders by mechanical alloying using high energy rate ball mill [9]. Magnetic properties and structure of nanocrystalline Fe-Al with Al content between 50 and 90 atomic % have been reported for low energy mechanical alloying of Fe and Al [10]. The intermetallic Fe_3Al has been successfully synthesized from the mixture of Fe and Al powders in a atomic ratio of 72 : 28 by mechanical alloying, structural evolution and nearest neighbour antiphase boundaries (NNAPBs) during alloying have been investigated [11]. None of these studies have reported high energy rate ball milling (MEA) under **toluene** solution. Thus, the objectives of the investigation have been synthesis, characterization, and study of mechanical and structural properties during MEA.

Fig. 1. High energy rate ball mill.

The **present work** was focused on the conventional mechanical alloying via high energy rate ball mill, nanostructured FeAl alloy powders were synthesized from elemental powders of Fe and Al. X-ray diffraction technique was used to investigate the phase transformation, changes in structural properties, atmospheric and milling media contamination during MEA. Scanning electron microscope (SEM) with EDS was employed to examine the morphology, particle size measurement and chemical analysis of mechanically alloyed powder. Vickers micro hardness (VMH) indentation test was carried out to study the hardness with respect to induced structural changes during MEA.

2. MATERIALS AND METHODS

2.1. High Energy Rate Ball Milling

Known as centrifugal or planetary mills (Fig. 1), these are devices used to rapidly grind materials to colloidal fineness, they develop high grinding energy via centrifugal or planetary action. To grind a sample in this device, the starting particle size should be less than 10 mm, the sample (material) and several balls are placed inside the bowl or jar and the balls to powder weight ratio depends on the type of material being ground and the fineness required. Bowl is mounted on an independent rotatable platform, the entire assembly of bowl, rotatable platform and the counter balancing weight are rotated in a direction opposite to the direction of the bowl rotatable platform, centrifugal forces alternately add and subtract.

Figure 2 shows jars and balls, these grinding media are available in different materials namely agate, sintered corundum, zirconium oxide, stainless steel, special steel, and tungsten carbide. For coarse particle size reduction large balls were used and ultra fineness requires the use of small balls, higher the ball density higher will be the pulverization energy. Pure elemental powders of Al and Fe were mechanically alloyed in a high energy rate planetary ball mill (Retsch PM-100) to obtain an average composition of Fe-50 atomic % Al. Initial particle size and purity of elemental powders was around 60 μm and 99.5% respectively. **Tungsten carbide** jar and balls were used, the ball to powder weight

Fig. 2. Grinding jars and balls.

ratio was 10:1. Jar and balls were cleaned to remove the coating from previous milling operations, running the ball mill with toluene solution cleans the balls and the jar. To minimize oxygen contamination, the milling process (mechanical alloying) was performed under **toluene** atmosphere. Elemental powders of Fe and Al in the desired quantity were ball milled under toluene fluid at 200 rpm and powder samples were collected at different ball milling duration (eg., 1/2 hr, 1 hr, 2 hrs, 3 hrs, –28 hrs).

2.2. Characterization

Jeol X-Ray diffractometer with a Cu K_α radiation ($\lambda = 0.1542$ nm) was utilised in investigating the structural and phase changes during MEA of the elemental powders. Furthermore, the investigation into the atmospheric and milling media contaminations was also performed by XRD. The lattice parameters were determined using at least three higher angle 20 peaks. The effective grain size, D, was calculated by averaging the results from applying the Scherrer formula (Eq. 1) to the first three diffraction peaks:

$$\beta_{\text{crystallite}} = k\lambda/D\cos\theta. \quad (1)$$

Where k is the Scherrer constant; λ is the wavelength of the incident radiation and θ is the Bragg angle. β, the full width at half maximum (FWHM) of the peaks, was obtained by subtracting the instrumental broadening using a fully annealed sample, β_i, from the observed broadening, β_0, using (Eq. 2):

$$\beta^2_{\text{cry}} = \beta^2_0 - \beta^2_i. \quad (2)$$

From XRD patterns, the relative long range order (LRO) parameter, S, was determined (Eq. 3) by a comparision of the relative intensities of superlattice ($h + k + l =$ odd) and fundamental ($h + k + l =$ even) peaks of nano powders (28 hr milled powder sample 221/110) with respect to the well annealed reference sample (100/110) according to:

$$S = \{(I_s/I_f)n/(I_s/I_f)r\}^{1/2}, \quad (3)$$

where I_s is the integrated intensity of the superlattice reflection peak, I_f is the integrated intensity of the fundamental, 110, peak, while "n" and "r" represent nano (28 hr milled) and reference samples respectively.

Jeol 6380 analytical **scanning electron microscope (SEM)** was utilised in particle size measurements and to study the morphology of the mechanically alloyed powder samples.

Energy dispersive X-ray spectroscopy (**EDS**) facility in the SEM was utilised to examine the chemical composition of the mechanically alloyed samples. The investigation into milling media and atmospheric contaminations were also done utilising the EDS facility.

2.3. Micro Hardness Testing

The Vicker's micro hardness (VMH) indentation tests were performed using Clemex computer controlled micro hardness tester. The powders were mounted in an epoxy cured at room temperature resin and were successively polished down to 0.3 μm. The tests were carried out by applying a load of 10 gm on single powder particle. Each micro hardness value shown in the results is the average of at least 5 measurements on different particles.

2.4. Indexing

Knowledge of crystal structure is a prerequisite to understand phenomena such as alloy formation and phase transformations. Indexing the pattern involves assigning the correct Miller indices to each peak in the diffraction pattern. When diffraction is present for unmixed *hkl* values (all odd or all even), then it can be concluded that the Bravais lattice is **fcc**. When reflections are present for $h + k + l =$ even, then the Bravais lattice is **bcc**. The Bravais lattice and the crystal structure are identified from the sequence of $h^2 + k^2 + l^2$ values in the diffraction pattern as shown in Table 1.

The XRD pattern of the sample ball milled for one hour duration is presented in Fig. 3, the pattern was recorded with Cu K_α radiation. Eight peaks exist in the diffraction pattern, and the 2θ values for these peaks are listed in Table 1. The $\sin^2\theta$ values have been calculated and the diffraction pattern was completely indexed as presented in the Table 1.

3. RESULTS AND DISCUSSION

3.1. XRD

XRD patterns of samples ball milled at different durations are shown in Fig. 3 to 6. For 1 hr milled sample, the fcc Al (200), (220), (222), (400) and (420) peaks superpose upon (110), (200), (211), (220) and

Table 1. Results of Indexing process on one hour ball milled sample

Peak	2θ	θ	$\sin^2\theta$	$\sin^2\theta/\sin^2\theta_{min}$	$h^2 + k^2 + l^2$	Unmixed (*hkl*) fcc Al	$h^2 + k^2 + l^2$ = even, bcc Fe
1	38.416	19.208	0.1082	1	3	(111)	–
2	44.632	22.316	0.1441	1.33	4	(200)	2 (110)
3	65.044	32.522	0.2890	2.67	8	(200)	4 (200)
4	78.16	39.08	0.3974	3.67	11	(311)	–
5	82.396	41.198	0.4338	4.00	12	(222)	6 (211)
6	99.148	49.574	0.5794	5.35	16	(400)	8 (220)
7	112.13	56.065	0.6883	6.36	19	(331)	–
8	116.788	58.328	0.7243	6.69	20	(420)	10 (310)

Table 2. Bragg angle and structural parameters for fundamental peaks and super lattice peak at different ball milling duration, contracted lattice parameter and crystallite size are 0.2869 nm and 18.32 nm respectively

Milling time, hr	2θ degrees	*hkl*	bcc/fcc	Phase	d Space in nm	"a" Lattice parameter, nm	"D" Crystallite size, nm	Fundamental/Super Lattice peak
0	38.52	111	fcc	Al		0.4044		elemental
0	44.73	110	bcc	Fe	0.2024	0.2862		elemental
1	44.62	110/200	bcc/fcc	Fe/Al	0.2030	0.2870/0.4060	25.68	Fundamental/elemental
12	44.56	110	bcc	Fe(Al)	0.2033	0.2875	22.44	Fundamental
18	44.5	110	bcc	Fe(Al)	0.2036	0.2879	19.95	Fundamental
28	44.656	110	bcc	FeAl	0.2029	0.2869	18.32	Fundamental
28	**71.308**	**221/300**	**bcc**	**FeAl**				**Super lattice**

(310) peaks of bcc Fe. The intensity of Al (111) peak is highest and Al (331) least among all the peaks in the diffraction pattern as shown in Fig. 3. From Table 2, for 1 hr milled sample, the Bragg angle of the superposed (110/200) peak is slightly less than that of unmilled bcc Fe, whereas the lattice parameter (0.2870 nm) obtained from this peak is greater than that of the unmilled Fe. These results suggest the beginning of the **phase trans-**

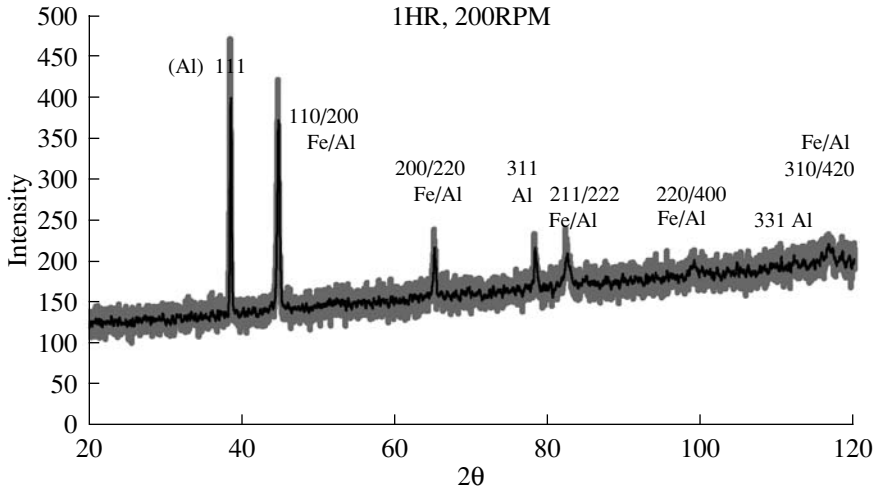

Fig. 3. XRD pattern of 1 hr milled sample, fcc Al (111) peak has the highest intensity among all the peaks, while among the superposed peaks Fe/Al (110/200) has the highest intensity.

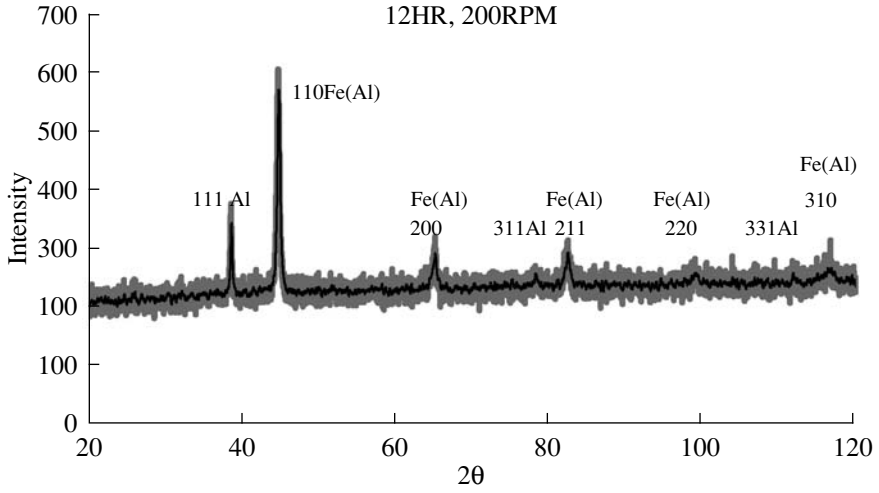

Fig. 4. XRD pattern of 12 hrs milled sample; the intensity of Al peaks decreased while that of fundamental peaks increased with peak broadening.

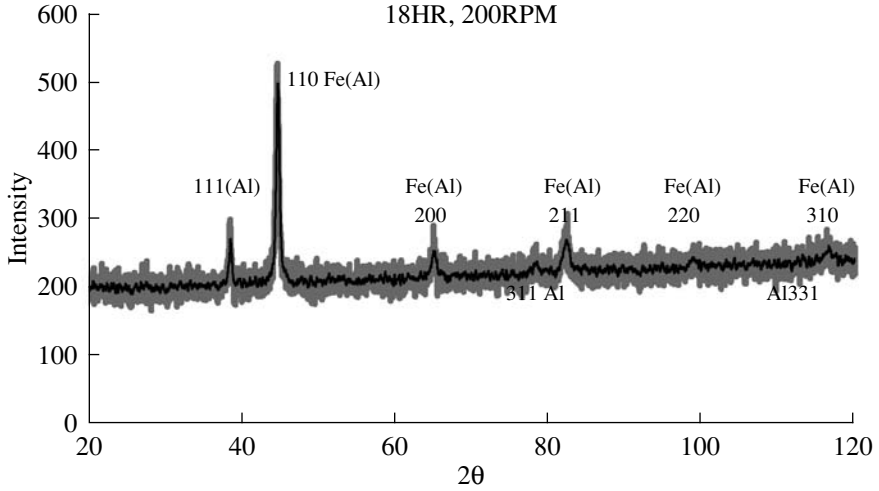

Fig. 5. XRD pattern for 18 hrs ball milled sample; decrease in intensity of Al peaks, fundamental peak broadening are further observed compared to the pattern of 12 hrs milled sample.

formation. The XRD pattern for 12 hrs milled sample from Fig. 4 shows the intensity of the strongest Al (111 and 311) peaks decreased compared to the pattern of one hr sample, the strongest Fe peak, (110), becomes the most intense one, slightly asymmetric, broadened and appears at a slightly lower Bragg angle. The decrease in the intensity of Al peaks indicate the diffusion of fcc Al atoms into bcc α Fe lattice, simultaneously peak shift to lower Bragg angles and asymmetric formation indicates the phase transformation from elemental phase to a disordered bcc Fe (Al) solid solution. Peak broadening is due to grain refinement, as seen from Table 2; the crystallite size reduces to around 22 nm. The intensity of bcc (110) peak is around 350 units, this increase in intensity compared to the pattern of 1 hr milled sample suggests the strong prevalence of Fe (Al) phase at the expense of elemental phase, the bcc (110) peak of Fe (Al) solid solution is known as fundamental peak. Asymmetric broadening of Fe peaks is mainly due to the formation of Fe (Al) solid solution and the unit cell parameter of such bcc solid solution are higher than that of pure Fe, Krasnowski M. et al. have shown such similar observations. Table 2 indicates that the lattice parameter obtained at the end of 12 hours of milling time is 0.2875 nm, which is greater than that of unmilled Fe and 1 hr milled sample. As milling time increases, separate Fe and Al phases are being replaced by a bcc Fe (Al) solid solution, hence the peaks of bcc Fe (Al) solid solution, the fundamental peaks ($h + k + l$ = even) are visible with greater intensities than the Al peaks as shown in Fig. 5 for 18 hrs milled sample. The Fig. 5 also shows fundamental peak broadening, shifting to lower Bragg angle and the absence of super lattice reflection ($h + k + l$ = odd).

Table 3. Indexed XRD pattern for ball milled sample of 28 hrs, notice the presence of super lattice reflection

Peak	2θ	θ	$\sin^2\theta$	$\sin^2\theta/\sin^2\theta_{min}$		$h^2 + k^2 + l^2$	Unmixed (*hkl*) fcc Al	$h^2 + k^2 + l^2$ = even, fundamental bcc, Fe (Al)	Super lattice peak, bcc (FeAl)
1	38.536	19.268	0.10889	1	× 3	3	111	–	–
2	44.656	22.328	0.14433	1.32	× 3	4	–	110	–
3	62.26	32.618	0.29055	2.66	× 3	8	–	200	–
4	**71.308**	**35.654**	**0.33975**	**3.12**	× 1	**9**	**–**	**–**	**221/300**
5	78.58	39.29	0.40100	3.68	× 3	11	311	–	–
6	82.3	41.15	0.43300	3.97	× 3	12	–	211	–
7	99.088	19.544	0.57897	5.31	× 3	16	–	220	–
8	**Absent**						**331**		–
9	116.404	58.202	0.72234	6.63	× 3	20	–	310	–

Peak shifting to lower Bragg angle as a function of milling time, points to an expansion of the bcc Fe lattice (0.2879 nm) during the alloying process as indicated in Table 2. Lattice expansion introduces antisite defects during the disorder as a function of milling time, i.e., both Fe and Al atoms are able to substitute each other's lattice, and the crystallite size obtained at the end of 18 hrs of milling is 19.95 nm. The absence of super lattice reflection proves the disordered structure of the solid solution, Q. Zeng et al. [12] have observed such variations in peak intensities, shift in Bragg angle, peak broadening and asymmetric formation and have interpreted it to be due to the migration of Al into Fe, formation of bcc Fe (A1) solid solution (A2) and crystallite size refinement. Table 3 shows the XRD indexing process for 28 hrs milled sample, notice the presence of super lattice peak.

Further diminishing of Al peaks, fundamental peak broadening and shift to higher Bragg angle are noticed for 28 hrs milled sample in Fig. 6. Observe the vanishing of Al (331) peak and the emergence of a low intensity bcc super lattice peak (221), these results indicate the transition from bcc Fe (Al) solid solution of disordered phase to FeAl ordered phase. Ordering phenomenon reduces the lattice parameter (0.2869 nm) and shifts the peak to higher Bragg angle as observed from the Table 2, the lattice contraction is due to annihilation of antisite defects resulting from diffusion over short distances and increased short range order. From the XRD data of the reference sample and the alloyed sample (milled for 28 hrs), the LRO parameter, *S*, is 0.49, indicates that the mechanically alloyed sample is partially ordered. M.A. Morris–Munoz et al. [13] have shown the formation of a partially ordered FeAl phase at longer milling duration. The presence of elemental Al peak at the end of 28 hours of MEA process as a

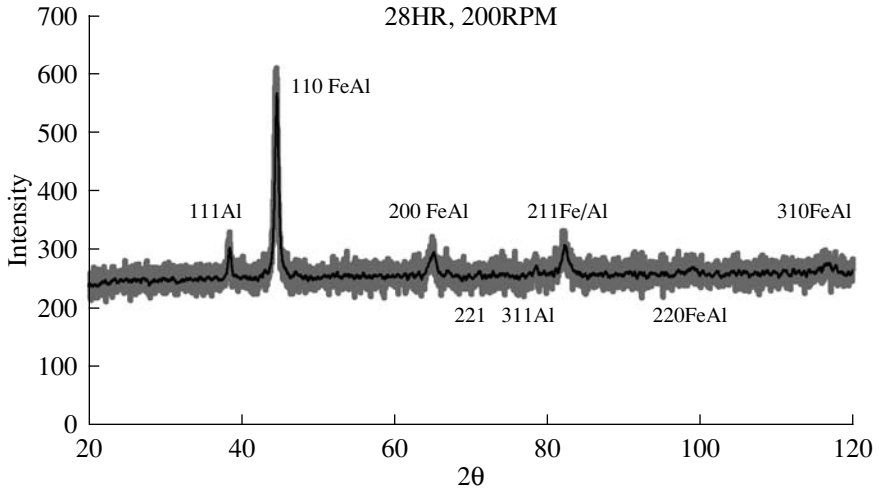

Fig. 6. Indexed XRD pattern for 28 hrs milled sample, low intensity bcc super lattice peak (221) is seen, further broadened fundamental peak and diminished Al peaks are observed, Al 331 peak is not seen.

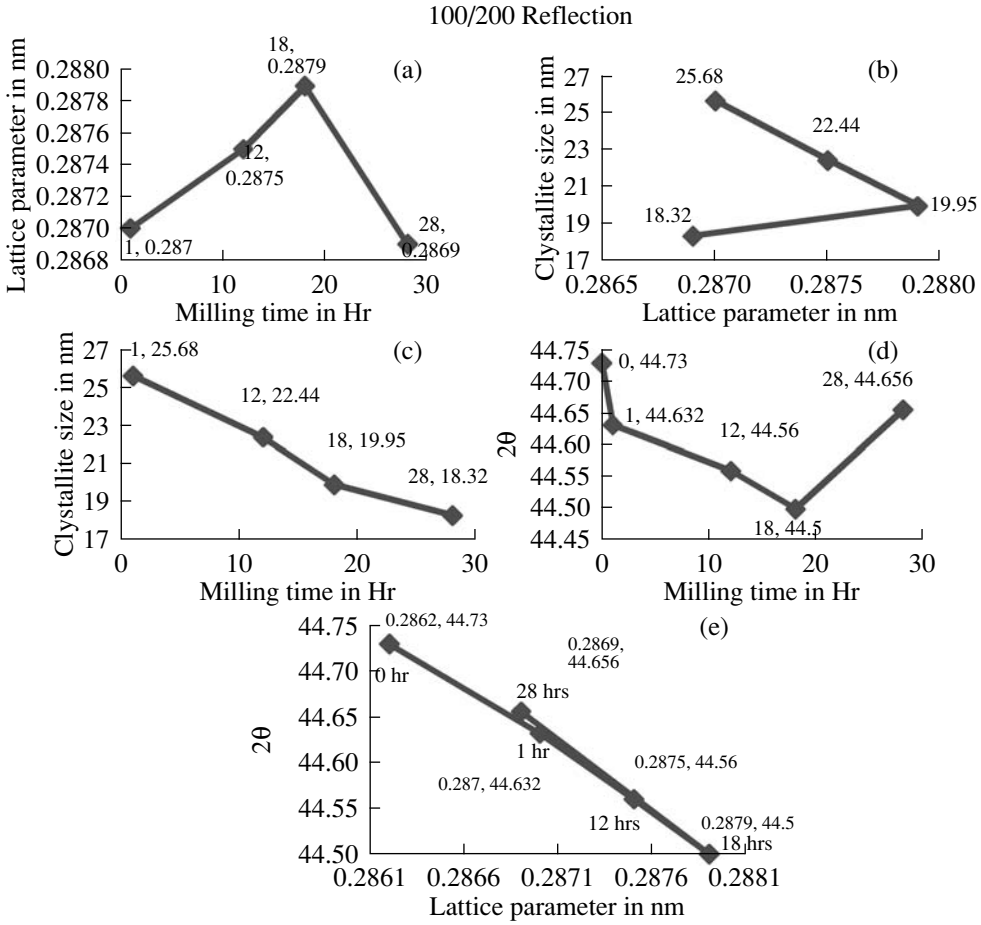

Fig. 7. (a) Lattice expansion occurs during 1 to 18 hrs of milling time, lattice contraction occurs during 18 to 28 hrs of milling time. (b) Crystallite size decreases from 25.68 nm to 19.95 nm during lattice expansion, while the decrease is from 19.95 nm to 18.32 nm during lattice contraction. (c) Crystallite size decrease is steep during 12 hrs to 18 hrs of milling time; it is due to stabilisation of disorder. (d) Bragg angle for the fundamental peak decreases from unmilled sample to 18 hrs milled sample, increase in Bragg angle occurs from 18 hrs to 28 hrs of milling time. (e) Bragg angle decreases during lattice expansion from 0.2862 nm to 0.2879 nm, while it increases during lattice contraction from 0.2879 nm to 0.2869 nm.

result of ball milling indicates the prevalence of two phases (elemental phase co exists with the alloyed phase).

The absence of $Fe_3Al(Do_3)$ peak around the Bragg angle of 26° confirms that the nanoparticle sample does not contain significant contamination from oxygen during the processing, furthermore, none of the XRD patterns show peaks of tungsten and carbon, suggesting negligible contamination from the milling media.

The lattice parameter increases from 0.2862 nm for unmilled Fe to 0.2879 nm for 18 hrs milled sample, this lattice expansion is shown in Fig. 7a, it is due to the formation of disordered Fe (Al) as explained earlier. The lattice contraction is accompanied by a transformation to an ordered FeAl phase. One of the possible reasons for fundamental peak broadening is crystallite size refinement, (Fig. 7b); lattice contraction is characterised by marginal decrease in crystallite size (19.95 nm to 18.32 nm) as compared to large reduction (25.68 to 19.95 nm) during lattice expansion. In Fig. 7c, the crystallite size decrease is steep during 12 hrs to 18 hrs of milling time; it is due to the disordered phase which prevails during MEA at this juncture. During disordering, the lattice expansion occurs, the entropy of the system is dominant and the atoms are located randomly in the bcc lattice of Fe (Al), leading to the formation of an antisite defect in the bcc lattice, thereby, increasing the chances of like atoms being the nearest neighbours, thus an atom occupying the wrong atomic site is possible. Such an arrangement of atoms causes the free energy of Fe (Al) to rise, thus the solid solution becomes thermodynamically metastable and offers very less resistance to grain refinement during the processing. In Figs. 7d and 7e, the peak is shifted to lower Bragg angle during milling to 18 hrs of time causing an expansion in lattice, whereas peak shift to higher Bragg angle for 28 hrs of milling time is followed by contraction in lattice parameter.

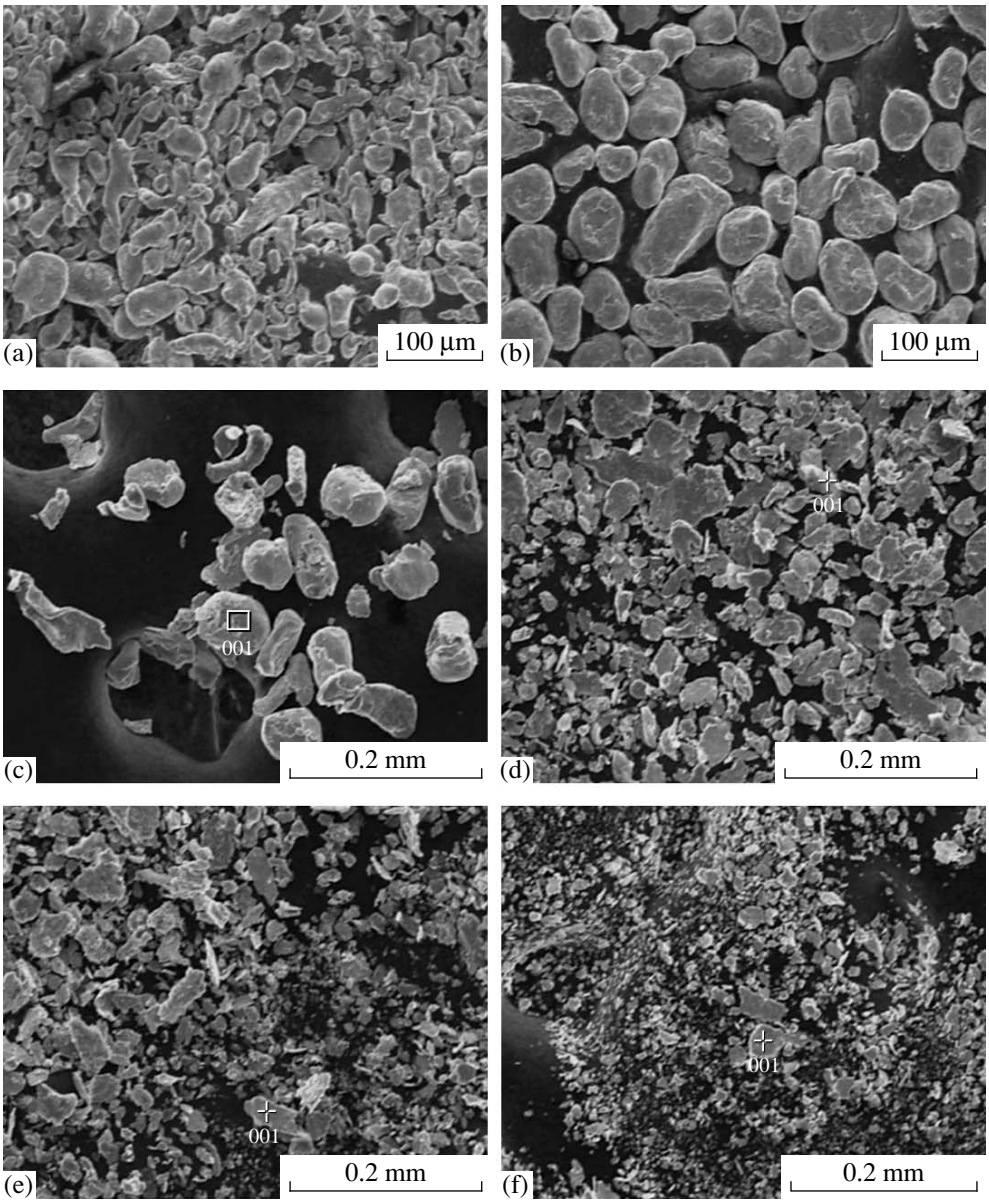

Fig. 8. SEM micrographs (a) Unmilled Al powders. (b) Unmilled Fe powders. (c) Ball milled for 1/2 hr. (d) Ball milled for 4 hrs. (e) Ball milled for 8 hrs. (f) Ball milled for 27 hrs.

3.2. SEM

SEM micrographs of unmilled powder samples are shown in Figs. 8a and 8b, the unmilled Fe powders were rounded while those of Al were elongated in shape. Figures 8c to 8f shows the sequence of SEM micrographs obtained at different milling duration; they illustrate the morphology of the powder particles ball milled from half an hour to 27 hrs. The average size of the powders gradually decreased with increasing milling time; it is also observed that the particle size distribution is wider at longer milling time. Welding and flattening of particles are observed during longer milling duration as seen from Figs. 8d to 8f.

3.3. EDS

SEM micrograph in Fig. 9a shows energy dispersive spectroscopy investigation on a particle mechanically alloyed for 18 hrs of time, approximately an average composition of Fe-50 at % Al is obtained as indicated

Table 4. Results of EDS performed using SEM on a mechanically alloyed particle

Elements	KeV	Mass %	Error %	Atomic %
Al Kα	1.486	29.43	0.17	46.33
Fe Kα	6.398	70.57	0.37	53.67
Total		100		100

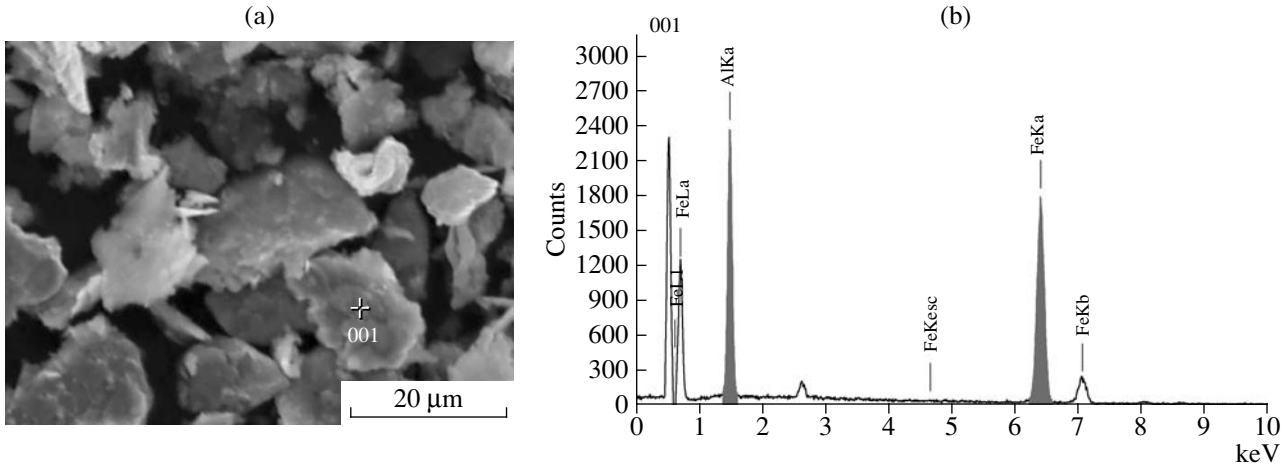

Fig. 9. (a) EDS micrograph shows spot analysis on a mechanically alloyed particle. (b) EDS graph indicates Fe and Al peaks.

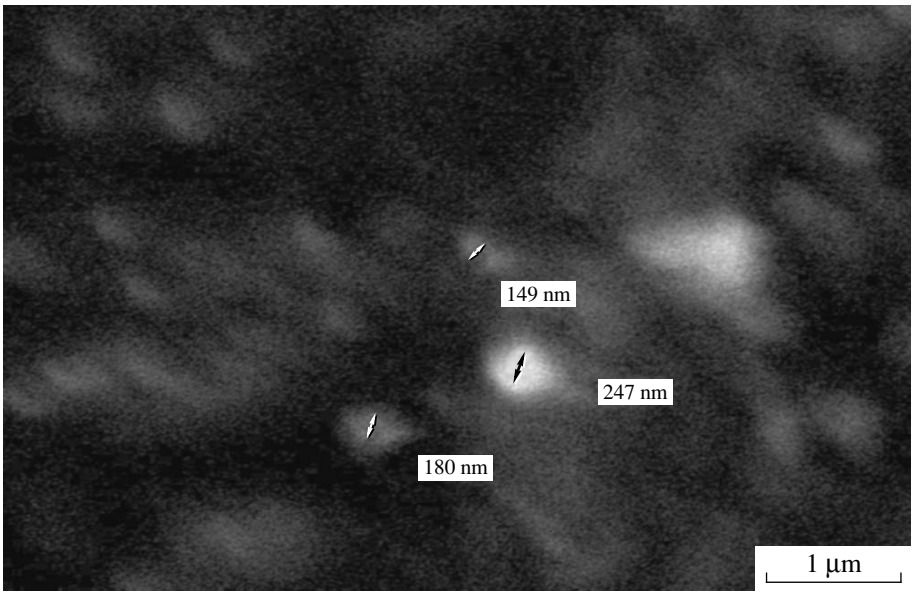

Fig. 10. SEM micrograph shows particle size measurement for 10 hrs milled sample.

in the Table 4. The EDS analysis showed only Fe and Al peaks, and no tungsten and carbon peaks are seen in Fig. 9b, suggesting negligible contamination from the atmosphere and the milling media. EDS and XRD results are similar with respect to phase transformation, particle size and contamination, thus showing consistency in the investigated results.

3.4. Particle Size Measurement

SEM micrograph in Fig. 10 reveals the particle size of ball milled powders; micrograph shows 149 nm sized particle, obtained for a milling duration of 10 hrs. Particle of 673 nm size is seen in the micrograph shown in Fig. 11, a number of minute particles much smaller than the 673 nm sized particle are visible, and these results indicate particle size reduction with increased milling time, leading to the formation of nanosized particles at longer milling duration.

3.5. Micro Hardness Test

It is a well known fact that the introduction of atoms into the solid solution produces an alloy, which is stronger than the pure metal. Following this approach, it can be inferred, that the mechanical properties of the mechanically alloyed intermetallics should be correlated to the induced structural changes, in particular the disorder to order transition. From Table 5 and Fig. 12a, it can be seen that the hardness increase is large during disordering (0 to 18 hrs of milling; when lattice expansion occurs). The hardness increase is marginal during

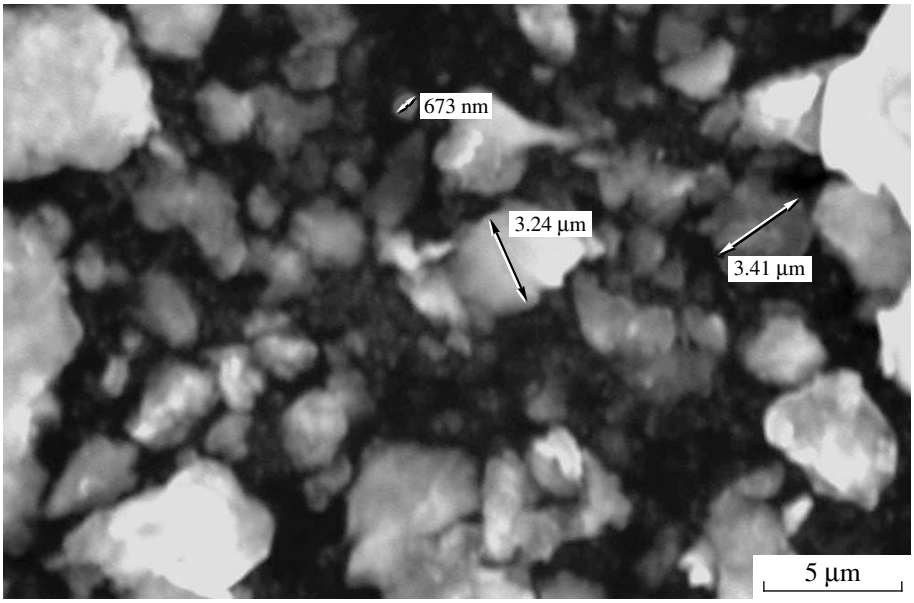

Fig. 11. SEM micrograph shows different particle sizes for a powder sample obtained at 24 hrs ball milling time.

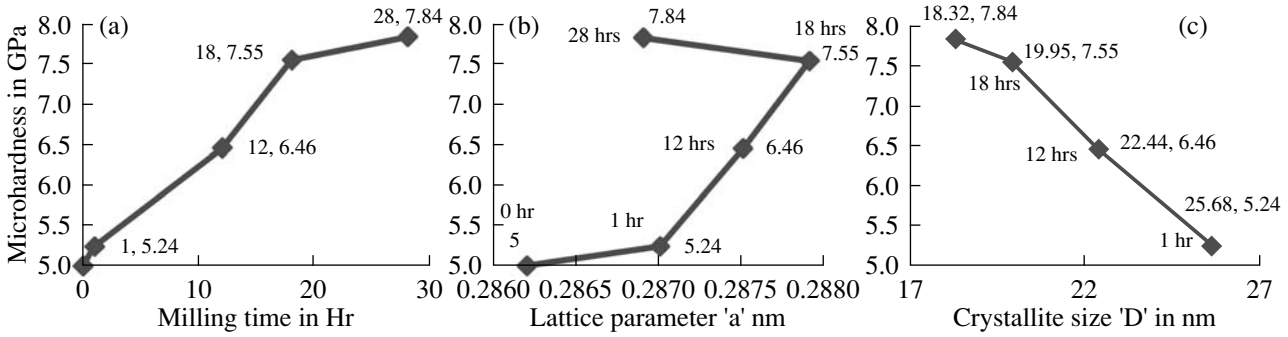

Fig. 12. (a) Micro hardness increases from 5.24 GPa to 7.55 GPa during disordering while the increase from 7.55 GPa to 7.84 GPa is due to ordering as a function of milling time. (b) Micro hardness increases from 5 GPa for unmilled sample to 7.84 GPa for 28 hrs milled sample, initial lattice expansion and final lattice contraction are observed with a marginal increase in hardness. (c) Hardness increases as crystallite size decreases, increase in hardness is small (7.55 GPa to 7.84 GPa) during ordering and large during disorder.

lattice contraction (7.55 to 7.84 GPa) as shown in Fig. 12b. The lattice contraction during ordering is accompanied by a softening of the material. The softening is related to marginal increase in hardness (7.55 GPa to 7.84 GPa) and small reduction in crystallite size (19.95 nm to 18.32 nm) as a result of ball milling (Fig. 12c), these changes would be mainly controlled by the concentration of antisite defects present in the alloy. Micro hardness increases with grain size reduction; hardness is not only enhanced by the disorder to order transition but also by the grain refinement. X. Amils et al. [14] and R.A. Varin et al. [15] have shown that the disordering process is characterized by an alloy hardening, which mainly depend on the grain refinement and the creation of antisite defects while the ordering process shows softening of the nanocrystalline alloy, which is governed by the annihilation of antisite defects.

4. CONCLUSIONS

Mechanically alloyed samples as a result of milling time of 18 hrs duration indicated, the bcc Fe peak broadening, slight asymmetric formation, and shift to

Table 5. Vickers micro hardness test results

Milling time in hr	Hardness value, GPa	Lattice parameter	Crystallite size "D"	*hkl* reflection
0	5	0.2862 nm	60–70 microns	110
1	5.24	0.2870 nm	25.68 nm	110/200
12	6.46	0.2875 nm	22.44 nm	110/200
18	7.55	0.2879 nm	19.95 nm	110/200
28	7.84	0.2869 nm	18.32 nm	110/200

slightly lower Bragg angle. Simultaneously the lattice parameter expanded, suggesting the formation of a new phase, the disordered bcc Fe (Al). The contraction of lattice parameter, peak shift to higher Bragg angle and broadening, coupled with the presence of super lattice peak have shown the transition to an ordered FeAl phase for ball milling duration of 28 hrs. The LRO parameter obtained suggests a partial ordering of the mechanically alloyed sample. The ordered structure obtained is characterised by a small decrease in crystallite size compared to large decrease during disordering. Formation of nanocrystallites was confirmed by the XRD peak broadening and the XRD estimated nanocrystallite size decreased from 26 nm after 1 hr to the 18 nm range after 28 hrs of milling. The presence of low intensity fcc Al peak along with the fundamental and super lattice peaks even after substantially long milling time, reveals that the process of MEA is still incomplete, complete alloy phase (Fe (Al) or FeAl) formation is prolonged due to milling under **toluene** solution. XRD results do not show DO_3, tungsten and carbon peaks, suggesting negligible contamination from the atmosphere and the milling media.

SEM micrographs showed particle size reduction leading to **nanoparticles** during MEA as a result of milling time. **EDS** analysis on a mechanically alloyed particle showed the atomic percentage of Fe and Al, thereby, confirming the formation of an alloy phase. Hardness increase is large during disordering and marginal during ordering; hardness is not only enhanced by the disorder to order transition but also due to grain refinement.

5. ACKNOWLEDGMENTS

The authors would like to acknowledge Dr. Surappa and Shri Krishnamurthy from the Materials Department at the Indian Institute of Science (IISc), Bangalore for providing the XRD facility.

REFERENCES

1. Negri et al., *Acta Mater.*, 1999, vol. 47, no. 18, pp. 4545–4554.
2. Rico, M.M. et al., *Journal of Alloys and Compounds*, 2005, vol. 398, pp. 26–32.
3. Oleszak, D. and Shingu, P.H., *Mater. Sci. Eng.*, 1994, vols. A 181, 182, pp. 1217–1221.
4. Huang, B. et al., *Mater. Sci. Eng.*, 1997, vol. A 231, pp. 72–79.
5. Eelman, D.A. et al., *J. Alloys Compd.*, 1998, vol. 266, pp. 234–240.
6. Hashii, M., *Mater. Sci. Forum*, 1999, vols. 312–314, pp. 139–144.
7. Krasnowski, M. et al., *Journal of Alloys and Comp.*, 2006, vol. 424, pp. 119–127.
8. Hongwei Shi et al., *Journal of Alloys and Comp.*, 2007, vol. 455, pp. 207–209.
9. Sebastian et al., *Intermetallics*, 2007, pp. 1–7.
10. Jartych, J. et al., *Nano Structured Materials*, 1999, vol. 12, pp. 927–930.
11. Run-Hua Fan et al., *Powder Tech.*, 2005, vol. 149, pp. 121–126.
12. Zeng, Q. and Baker, I., *Intermetallics*, 2006, vol. 14, pp. 396–405.
13. Morris–Munoz, M.A. et al., *Nano Structured Materials*, 1999, vol. 11, no. 7, pp. 873–885.
14. Amils, X. et al., *Nano Structured Materials*, 1999, vol. 11, no. 6, pp. 689–695.
15. Varin, R.A. et al., *Materials Science and Engineering*, 2002, vols. A 329–331, pp. 213–221.